

# LAMINAR FORCED CONVECTION FROM ISOTHERMAL RECTANGULAR PLATES FROM SMALL TO LARGE REYNOLDS NUMBERS

M.M. Yovanovich<sup>†</sup> and P. Teertstra<sup>‡</sup>  
Microelectronics Heat Transfer Laboratory  
Department of Mechanical Engineering  
University of Waterloo  
Waterloo, Ontario, Canada N2L 3G1  
<http://www.mhtl.uwaterloo.ca>

## Abstract

A composite model for area-average Nusselt number for forced, laminar flow parallel to finite, isothermal rectangular plates for a wide range of Reynolds numbers is proposed. The correlation equation is based on the superposition of the dimensionless shape factor and a modified laminar flow boundary layer asymptote with an empirically determined interpolation parameter. The Nusselt and Reynolds numbers and the dimensionless shape factor are based on either the rectangle side dimension parallel to the flow direction or the square root of the heat transfer area. The proposed correlation equations are applicable to rectangles with side dimension ratios in a range from 1 to 10. Extensive numerical results were used to find the optimal values of the interpolation parameter to provide close agreement between the correlation equation predictions and the numerical values.

## Nomenclature

$A$	=	plate surface area, $\equiv L \times W$ , $m^2$
$C, C_T$	=	boundary layer solution coefficients
$F(Pr)$	=	Prandtl number function, Eq. (17)
$h$	=	convective coefficient, $W/m^2K$
$k$	=	thermal conductivity, $W/mK$
$L$	=	long plate dimension, $m$
$\mathcal{L}$	=	general scale length, $m$

$n$	=	interpolation parameter, Eq. (21), or normal unit vector, Eq. (9)
$Nu_{\mathcal{L}}$	=	Nusselt number, $\equiv \frac{Q\mathcal{L}}{kA(T_w - T_\infty)}$
$Pr$	=	Prandtl number
$Q$	=	heat flow rate, $W$
$Q_{\mathcal{L}}^*$	=	dimensionless heat transfer rate, $\equiv \frac{Q\mathcal{L}}{kA(T_w - T_\infty)}$
$Re_{\mathcal{L}}$	=	Reynolds number, $\equiv \frac{U_\infty \mathcal{L}}{\nu}$
$Re_{\sqrt{A}}^*$	=	modified Reynolds number, Eqs. (29, 30)
$S^*$	=	dimensionless conduction shape factor
$T_w$	=	plate surface temperature, $^\circ C$
$T_\infty$	=	ambient temperature, $^\circ C$
$U_\infty$	=	free stream velocity, $m/s$
$u, v, w$	=	velocity components, $m/s$
$W$	=	short plate dimension, $m$
$x, y, z$	=	Cartesian coordinates
$X, Y, Z$	=	computational domain size, $m$

### *Greek Symbols*

$\alpha$	=	thermal diffusivity, $m^2/s$
$\phi$	=	dimensionless temperature, $\equiv \frac{T - T_\infty}{T_w - T_\infty}$
$\nu$	=	kinematic viscosity, $m^2/s$

### *Subscripts*

$\sqrt{A}$	=	with square root of plate area $A$
$L$	=	with long plate dimension
$w$	=	plate surface
$W$	=	with short plate dimension
$\infty$	=	free stream

---

<sup>†</sup> Fellow, AIAA

<sup>‡</sup> Graduate Research Assistant

Copyright ©1998 by the authors. Published by the American Institute of Aeronautics and Astronautics, Inc. with permission.

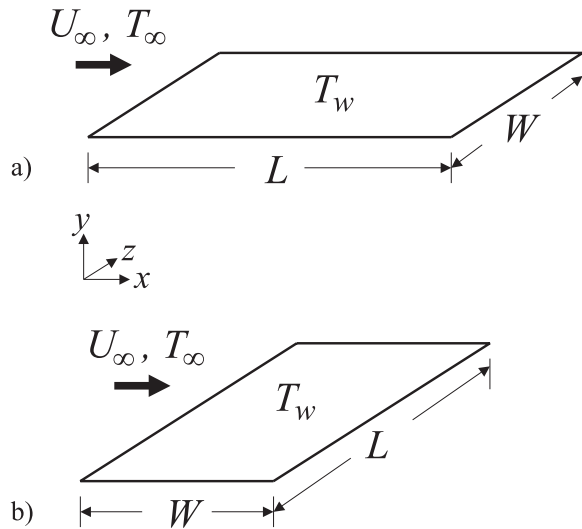


Fig. 1 Schematics of physical problem:  
a) flow along long plate dimension  $L$   
b) flow along short plate dimension  $W$

## Introduction

Laminar forced convective heat transfer from isothermal finite rectangular plates (shown in Fig. 1) over a large range of Reynolds number such as  $1 \leq Re \leq 5000$  is of considerable interest for modeling the thermal performance of microelectronic systems. A review of the open literature shows that this problem has not been addressed fully. Correlation equations<sup>1-4</sup> are available for the local and area-average Nusselt number for all Prandtl numbers and for a limited range of the Reynolds number, such as  $100 < Re < 10^5$ . The correlation equations are limited to two-dimensional laminar boundary layer flow, and therefore they cannot be used for finite plates at small Reynolds numbers, where thermal diffusion becomes very important and the resulting temperature field is three-dimensional.

A recent publication<sup>5</sup> presented a composite model for the Nusselt number which is reported to be valid for a wide range of Reynolds and Prandtl numbers. The correlation equation includes the diffusive limit for zero fluid flow and the boundary layer limit which accounts for turbulent effects. The composite model is based on the linear superposition of the two limits, and the scale length used in the Nusselt and Reynolds numbers, and the shape factor is based on the square root of the total surface area. However, this model is limited to two-dimensional

boundary layer flow and is therefore not applicable to the finite rectangular plate problem.

The major objectives of this paper are as follows: i) to present the development of a composite correlation equation that will accurately predict the average Nusselt number for all fluids  $Pr > 0.5$ , and for a wide range of the Reynolds number,  $0 < Re_{\mathcal{L}} < 5000$ ; ii) to examine the effect of the scale length used in the dimensionless parameters such as the Nusselt and Reynolds numbers and the shape factor; and iii) to report accurate numerical values of the Nusselt number for the finite rectangular plate over a wide range of the Reynolds number and aspect ratio.

## Physical Problem Description

Consider steady, laminar flow of a constant property fluid of large extent and temperature  $T_{\infty}$  parallel to a finite isothermal rectangular plate of zero thickness and side dimensions  $L$  and  $W$  where  $L/W \geq 1$ . The upper surface is maintained at temperature  $T_w$  and the lower surface of the plate is assumed to be adiabatic. The total heat transfer area is therefore  $A = LW$ . Two flow cases are considered as shown in Fig. 1: a) flow parallel to the longer side dimension  $L$  and b) flow parallel to the shorter side dimension  $W$ . The ratio of the side dimensions of the rectangular plate ranges between 1 for the square plate to 10 for a long rectangular plate. The Reynolds number based on the free stream velocity  $U_{\infty}$  and the plate dimension parallel to the flow direction will range from 0.1 up to about 5000. The local heat flux distribution over the surface of the isothermal plate is highly distributed. When the Reynolds number is very small, the heat flux attains its maximum values along the four edges of the rectangular plate. For larger values of the Reynolds number the maximum values of the local heat flux occur along the leading edge where the fluid first encounters the plate. As the Reynolds number increases from small to large values the flux distribution changes significantly between the two cases described above.

## Mathematical Problems

The governing differential equations in vector form for the full three-dimensional problem are the continuity equation:

$$\nabla \cdot \vec{V} = 0 \quad (1)$$

the momentum equation for zero pressure gradient along the plate surface:

$$\nu \nabla^2 \vec{V} = (\vec{V} \cdot \nabla) \vec{V} \quad (2)$$

and the thermal energy equation with negligible viscous heating:

$$\alpha \nabla^2 T = (\vec{V} \cdot \nabla) T \quad (3)$$

where the Laplacian operator in Cartesian coordinates is:

$$\nabla^2 = \frac{\partial^2}{\partial x^2} + \frac{\partial^2}{\partial y^2} + \frac{\partial^2}{\partial z^2} \quad (4)$$

The constant thermophysical properties which appear in the momentum and energy equations are the kinematic viscosity  $\nu$  and the thermal diffusivity  $\alpha$ , respectively. It has been assumed that there is negligible viscous heating because the flow velocity is sufficiently small. There are no analytical solutions of the Navier-Stokes equations for the full range of the Reynolds number from small values,  $Re_{\mathcal{L}} = 0$ , to large values,  $Re_{\mathcal{L}} = 5000$ . When the Reynolds number lies in the range  $100 < Re_{\mathcal{L}} < 10^5$  the flow is considered to be laminar and the hydrodynamic boundary layer thickness is much smaller than the plate side dimension parallel to the flow. In the case of high Prandtl number fluids, the thermal boundary layer is smaller than the hydrodynamic boundary layer thickness, and the Navier-Stokes equations reduce to the boundary layer two-dimensional forms for the continuity equation:

$$\frac{\partial u}{\partial x} + \frac{\partial v}{\partial y} = 0 \quad (5)$$

the momentum equation:

$$\nu \frac{\partial^2 u}{\partial y^2} = u \frac{\partial u}{\partial x} + v \frac{\partial u}{\partial y} \quad (6)$$

and the energy equation:

$$\alpha \frac{\partial^2 T}{\partial y^2} = u \frac{\partial T}{\partial x} + v \frac{\partial T}{\partial y} \quad (7)$$

where  $u$  and  $v$  are the velocity components along the  $x$ - and  $y$ -coordinates, respectively. When the Reynolds number approaches very small values such as  $Re_{\mathcal{L}} < 0.1$ , the solution of the energy equation will approach the solution of the three-dimensional Laplace equation:

$$\nabla^2 T = 0 \quad (8)$$

For all problems the dimensionless heat transfer rate from the surface of the isothermal rectangular plate is obtained from the relation:

$$Q_{\mathcal{L}}^* = \frac{Q\mathcal{L}}{kA(T_w - T_{\infty})} = \frac{\mathcal{L}}{A} \iint_A -\frac{\partial \phi}{\partial n} dA \quad (9)$$

where  $Q$  is the total heat transfer rate from the plate,  $\mathcal{L}$  is some characteristic scale length,  $A$  is the total surface area,  $k$  is the thermal conductivity, and  $T_w$  and  $T_{\infty}$  are the temperatures of the plate and the fluid at points remote from the center of the plate. The dimensionless temperature is  $\phi = (T(x, y, z) - T_{\infty}) / (T_w - T_{\infty})$  and  $n$  represents the surface normal directed into the fluid for all points in the surface of the plate. The thermal and hydrodynamic boundary conditions for all points in the surface of the plate are  $T = T_w$  and  $u = v = w = 0$ . At points remote from the center of the plate  $T \rightarrow T_{\infty}$  and  $u \rightarrow U_{\infty}$ , and both velocity components  $v$  and  $w$  go to 0.

## Solutions of the Limiting Problems

Analytical solutions to the full equations for arbitrary values of the Reynolds number are not available. Results of the available analytical and numerical solutions for limiting cases of the full equations are considered below. These relations will be used in subsequent sections to develop a composite model for the dimensionless heat transfer rate over a wide range of the Reynolds number.

### Diffusive Limit Solution

The dimensionless heat transfer rate for zero velocity (called the diffusive limit) is obtained from the solution of the three-dimensional Laplace equation. The dimensionless heat transfer rate for this limit is called the dimensionless shape factor<sup>6</sup>, defined as:

$$Q_{\mathcal{L}}^* = S_{\mathcal{L}}^* = \frac{S\mathcal{L}}{A} \quad (10)$$

for the limit  $Re_{\mathcal{L}} \rightarrow 0$ . Analytical solutions for the conduction shape factor for the isothermal rectangular plate are currently not available; however Yovanovich<sup>6</sup> has shown that the analytical solution for the isothermal elliptical disk can be used to approximate the numerical results<sup>7</sup> for the isothermal rectangular plate with acceptable accuracy. This approximate solution requires that the heat transfer areas and the aspect ratios of the rectangular plate and the elliptical disk are similar, and the characteristic scale length is based on the square root of the total active area. The recommended relations for the dimensionless shape factor for the isothermal rectangular plate are<sup>6</sup>:

$$S_{\sqrt{A}}^* = \frac{(1 + \sqrt{L/W})^2}{\sqrt{\pi L/W}}, \quad 1 \leq L/W \leq 5 \quad (11)$$

and

$$S_{\sqrt{A}}^* = \frac{2\sqrt{\pi L/W}}{\ln(4L/W)}, \quad 5 < L/W < \infty \quad (12)$$

The dimensionless shape factor depends weakly on the rectangle aspect ratio  $L/W \geq 1$  when  $\mathcal{L} = \sqrt{A}$ . The maximum difference between the predicted values and previously determined numerical values<sup>7</sup> for the range:  $1 \leq L/W \leq 4$  is less than 1%. It is expected that the two relations should provide values which are within  $\pm 3\%$  of the numerical estimates for larger values of  $L/W$ . When the side length dimensions  $L$  or  $W$  are selected as the length scale, the dimensionless shape factors are obtained from:

$$S_L^* = \sqrt{\frac{L}{W}} S_{\sqrt{A}}^* \quad (13)$$

and

$$S_W^* = \sqrt{\frac{W}{L}} S_{\sqrt{A}}^* \quad (14)$$

### Boundary Layer Solutions

The two-dimensional boundary layer equations were solved by Blasius<sup>1</sup> and Pohlhausen<sup>1</sup>, and these solutions are well-documented in all fluids and heat transfer texts<sup>1-4</sup>. For laminar flow over an isothermal plate of length  $L$ , the area-average Nusselt number for  $Pr > 0.5$  and  $100 < Re_L < 10^5$  is given by the relation:

$$Nu_L = C Re_L^{1/2} Pr^{1/3} \quad (15)$$

where the most frequently quoted value for the coefficient is  $C = 0.664$ . According to Kays and Crawford<sup>3</sup>, the true value of the coefficient for the  $Pr \rightarrow \infty$  limit is  $C = 0.677$ .

Yovanovich et al.<sup>8</sup> obtained an approximate analytical solution which is based on a linearization of the momentum and energy equations. They reported that the area-average Nusselt number can be obtained from the relation:

$$Nu_L = 2 F(Pr) Re_L^{1/2} \quad (16)$$

where the Prandtl number function is defined as:

$$F(Pr) = \left[ \frac{Pr}{\pi [1 + (C_T Pr^{1/3})^2]^{1/2}} \right]^{1/2} \quad (17)$$

which is valid for  $0 < Pr < \infty$ . The limiting values of the Prandtl number function were reported as:

$$F(Pr) \rightarrow \frac{1}{\sqrt{\pi}} \sqrt{Pr}, \quad Pr \rightarrow 0 \quad (18)$$

and

$$F(Pr) \rightarrow \frac{1}{\sqrt{\pi C_T}} Pr^{1/3}, \quad Pr \rightarrow \infty \quad (19)$$

in complete agreement with the analytical result<sup>1-4</sup>.

The numerical value of the constant  $C_T$  which appears in the linearized energy equation can be determined in two ways. By matching the wall heat flux of the proposed linearized model against the value obtained from the Pohlhausen solution, a value of  $C_T = 2.77$  is obtained. Matching the enthalpy flux into the thermal boundary layer predicted by the proposed model against the value obtained by means of the integral energy equation solution results in a lower value of the coefficient,  $C_T = 2.13$ . By assuming a value of  $C_T = 2.31$ , which is close to various averages of these two values, the linearized model gives a boundary layer solution identical in form to the Pohlhausen solution except for a larger coefficient,  $C = 0.742$ .

### Proposed Composite Model

The proposed model consists of two components, the laminar boundary layer solution and the solution for thermal diffusion. The laminar boundary layer solution has the form:

$$Nu_{\mathcal{L}} = 0.742 Re_{\mathcal{L}}^{1/2} Pr^{1/3} \quad (20)$$

which is valid for  $Pr > 0.5$  and  $100 < Re_{\mathcal{L}} < 10^5$ . In the proposed boundary layer solution the Nusselt and Reynolds numbers are based on the arbitrary scale length  $\mathcal{L}$ . The conventional characteristic length used in the Nusselt and Reynolds numbers is the length of the plate in the flow direction,  $L$  or  $W$ . The appropriate length scale will arise from the subsequent analysis.

The proposed composite correlation equation is based on the Churchill-Usagi<sup>9</sup> method of combining asymptotic solutions:

$$Nu_{\mathcal{L}} = \left[ (S_{\mathcal{L}}^*)^n + \left( 0.742 Re_{\mathcal{L}}^{1/2} Pr^{1/3} \right)^n \right]^{1/n} \quad (21)$$

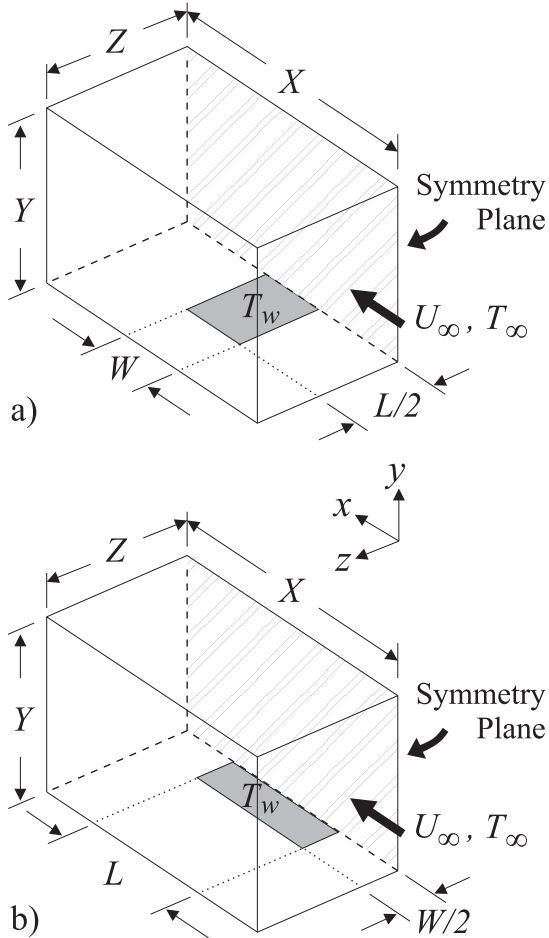


Fig. 2 Schematics of CFD solution domain:  
a) flow along short plate dimension  $W$   
b) flow along long plate dimension  $L$

where the interpolation parameter  $n$  ensures that the model predicts accurate values of the Nusselt number for intermediate values of the Reynolds number. The interpolation parameter is expected to be dependent on the aspect ratio of the rectangular plate when the conventional length scales are used in the Nusselt and Reynolds numbers and the dimensionless shape factor. The appropriate values of this parameter will be found by fitting the proposed model to numerical values obtained by means of a well-established commercial CFD code.

## Numerical Procedure

The analytical forced convection model developed in the previous section was validated and optimized using results obtained from simulations performed using FLOTHERM<sup>10</sup>, a commercial finite

volume based CFD software package. These CFD simulations were used to model the fluid flow and heat transfer within an air-filled region surrounding the isothermal plate, as shown in Fig. 2.

The flat plate was modelled as an isothermal, no-slip boundary in contact with the moving fluid, and symmetry was applied in the streamwise direction as shown in the Fig. 2. The uniform free stream velocity  $U_\infty$  and ambient temperature  $T_\infty$  were specified at the upstream boundary, and the downstream and lateral domain boundaries were set to atmospheric (zero) pressure, allowing heat and mass to exit freely from the system. The plate and ambient air temperatures were set to  $T_w = 40^\circ\text{C}$  and  $T_\infty = 20^\circ\text{C}$ , respectively, and constant air properties evaluated at the film temperature  $300\text{K}$  were assumed.

Because of the large range of Reynolds number proposed for these simulations,  $1 \leq Re \leq 5000$ , it was anticipated that different computational domain sizes would be required, depending on the Reynolds number. For small Reynolds number,  $Re < 10$ , the heat transfer is dominated by conduction, requiring a large computational domain to model a fluid region of infinite extent. This same solution domain is also valid for the diffusive limit, the limiting case when  $Re \rightarrow 0$ , where heat transfer is by conduction only. At the large Reynolds number limit,  $Re_L > 1000$ , the majority of the heat transfer from the plate is by convection through a thin laminar boundary layer. At this limit, the size of the domain can be substantially reduced, but many more control volumes concentrated near the plate surface are necessary to accurately resolve the large temperature gradients.

The dimensions of the solution domain in the  $x$ -,  $y$ - and  $z$ -directions are characterized by  $X$ ,  $Y$  and  $Z$ , respectively, as shown in Fig. 2. Typical values for these dimensions used in the CFD simulations, non-dimensionalized using the plate length  $L$ , are presented in Table 1.

In order to generate accurate results using the CFD model, it is necessary to demonstrate that the

Table 1 Typical CFD solution domain dimensions

$Re$	$X/L$	$Y/L$	$Z/L$
$\rightarrow 0$	100	50	50
1	100	50	50
10	100	50	50
100	50	20	20
1000	15	1.5	7

Table 2 Summary of test cases for CFD simulations

$L/W$	Flow Direction	$Re$
10	$W$	$\rightarrow 0, 1, 10, 100, 500$
5	$W$	$\rightarrow 0, 1, 2, 4, 10, 20, 40, 100, 200, 400, 1000$
2	$W$	$\rightarrow 0, 1, 2.5, 5, 10, 25, 50, 100, 250, 500, 1000, 2500$
1	$L$	$\rightarrow 0, 1, 2, 5, 10, 20, 50, 100, 200, 500, 1000, 2717.3, 5000$
2	$L$	$\rightarrow 0, 1, 2, 5, 10, 20, 50, 100, 200, 500, 1000, 2000, 5000$
5	$L$	$\rightarrow 0, 1, 2, 5, 10, 20, 50, 100, 200, 500, 1000, 2000, 5000$
10	$L$	$\rightarrow 0, 1, 10, 100, 1000$

effect of the size and number of control volumes on the solution have been minimized. Because of the distinct differences between the models for small and large  $Re$ , two grid convergence studies were performed.

For the square plate with  $Re = 2717.3$ , two test cases were examined. The refined grid used in the second case had a 5.3 times increase in the number of control volumes over the first, to 144,000, and a 60% reduction in the thickness of the first layer of control volumes in contact with the plate surface. The resulting change in Nusselt number was only 0.5%, indicating that a converged solution had been achieved. The finer grid from the second test case was used for all remaining large  $Re$  simulations.

The second grid convergence study involved two test cases for the diffusive limit for  $L/W = 5$  with flow parallel to the long side length  $L$ . The finer grid in the second case had a 3.3 times increase in the number of control volumes, to 745,000, and a 40% reduction in the thickness of the first layer of control volumes in contact with the plate surface. The resulting change in  $Nu$  was 2.4%, and the result from the finer grid was within 0.6% of the value predicted by the available analytical expression, Eq. (13).

## Numerical Results and Discussion

With the size and discretization of the computation domain established, the CFD model was used to simulate a wide range of aspect ratios and Reynolds

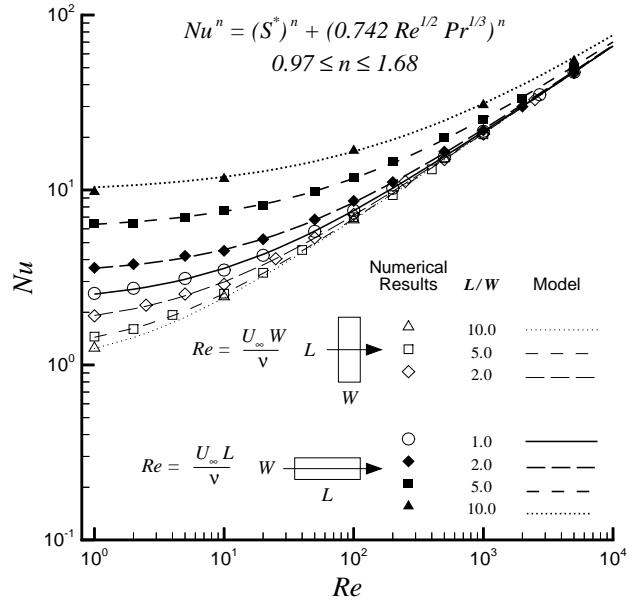


Fig. 3 Comparison of data and model with  $L$  and  $W$  as characteristic length

numbers, for both flow along the long plate dimension  $L$  and the short plate dimension  $W$ , as shown in Table 2.

The numerical results for these test cases are compared with the predictions of the proposed model, Eq. (21), in Fig. 3. The data are non-dimensionalized using Nusselt and Reynolds numbers defined as follows. For the bulk velocity parallel to the short plate dimension  $W$ :

$$Nu = Nu_W = \frac{QW}{kA(T_w - T_\infty)} \quad (22)$$

$$Re = Re_W = \frac{U_\infty W}{\nu} \quad (23)$$

and for flow parallel to the long plate dimension  $L$ :

$$Nu = Nu_L = \frac{QL}{kA(T_w - T_\infty)} \quad (24)$$

$$Re = Re_L = \frac{U_\infty L}{\nu} \quad (25)$$

The data are compared with the following form of the proposed model:

$$Nu = \left[ (S^*)^n + (0.742 Re^{1/2} Pr^{1/3})^n \right]^{1/n} \quad (26)$$

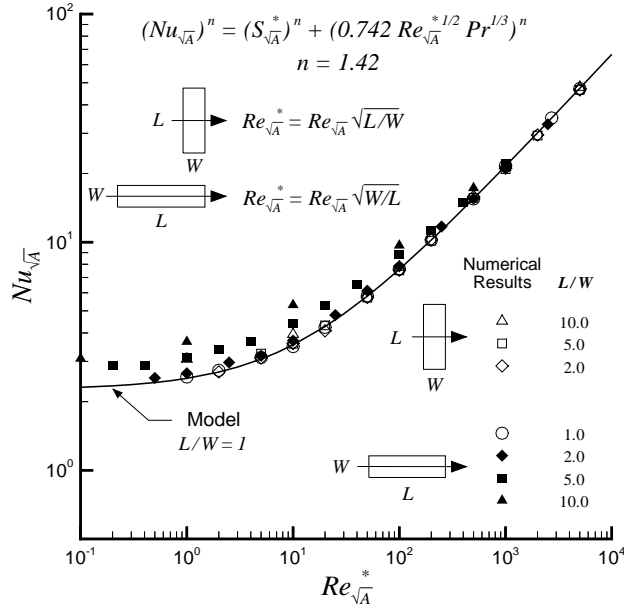


Fig. 4 Comparison of data and model with  $\sqrt{A}$  as characteristic length

where  $Nu$  and  $Re$  are defined in Eqs. (22 - 25). The conduction shape factor  $S^*$  is determined by Eq. (14) for flow along the short plate dimension  $W$  and by Eq. (13) for flow parallel to  $L$ .

Using the numerical data, optimized values for the interpolation parameter  $n$  were determined which minimized the deviation between the proposed model and the data. The resulting interpolation parameters for all test cases vary according to aspect ratio and flow direction in the range:

$$0.97 \leq n \leq 1.68$$

These optimized values for the interpolation parameter  $n$  were correlated separately for each flow direction as a function of the aspect ratio. For bulk velocity parallel to the short plate dimension  $W$ :

$$n = 1.42 - 0.28 \log_{10}(W/L) \quad (27)$$

and for flow along the long plate dimension  $L$ :

$$n = 1.42 - 0.45 \log_{10}(L/W) \quad (28)$$

For the square plate where  $L = W$ , both correlation equations provide identical values.

Using the proposed model, Eq. (26), and the interpolation parameter  $n$  from the appropriate correlation equation, Eq. (27) or (28), the numerical

results are predicted within a maximum percent difference of 4.5% and an RMS percent difference of 1.9%.

The large variation in the values of the interpolation parameter for the different aspect ratio and flow direction cases can be attributed to the use of the plate dimensions  $L$  or  $W$  as the characteristic length in the dimensionless quantities  $Nu$ ,  $S^*$  and  $Re$ . From Fig. 3 it is seen that for large  $Re$ , the Nusselt number becomes independent of the aspect ratio and flow direction and approaches a single asymptote, corresponding to the two-dimensional boundary layer solution described previously. However, for small values of  $Re$  there is an order of magnitude difference between the results for  $L/W = 10$  when the flow is in the  $L$  and  $W$  direction. These differences in the diffusive limit change the shape of the  $Nu$  vs.  $Re$  curves, requiring different interpolation parameters for the model to properly fit the data.

Previous research (Yovanovich<sup>6</sup>) has shown that the use of the square root of the active surface area of the body as the characteristic length can reduce the variation of the results as a function of aspect ratio. In addition the diffusive limit, Eqs. (11) and (12), is independent of the flow direction when  $\sqrt{A}$  is used as the characteristic length.

The data are recast using  $\sqrt{A}$  as the characteristic length, and the results, expressed as  $Nu_{\sqrt{A}}$  are plotted as a function of  $Re_{\sqrt{A}}^*$  in Fig. 4. The modified Reynolds number  $Re_{\sqrt{A}}^*$  has been introduced to account for flow direction effects in the boundary layer solution. For bulk velocity parallel to the short dimension of the plate  $W$ , this modified Reynolds number is defined as:

$$Re_{\sqrt{A}}^* = Re_{\sqrt{A}} \cdot \sqrt{L/W} \quad (29)$$

and for flow along the long plate dimension  $L$ :

$$Re_{\sqrt{A}}^* = Re_{\sqrt{A}} \cdot \sqrt{W/L} \quad (30)$$

The proposed model is recast in a similar manner:

$$Nu_{\sqrt{A}} = \left[ \left( S_{\sqrt{A}}^* \right)^n + \left( 0.742 Re_{\sqrt{A}}^{*1/2} Pr^{1/3} \right)^n \right]^{1/n} \quad (31)$$

Equation (31) is plotted in Fig. 4 for the square plate,  $L = W$ . Because the results for the square plate are unaffected by recasting the model in terms of  $\sqrt{A}$ , the interpolation parameter  $n = 1.42$  used previously is retained.

From Fig. 4 it is seen that the variation between the data for different aspect ratios and flow directions has been reduced significantly. The data for

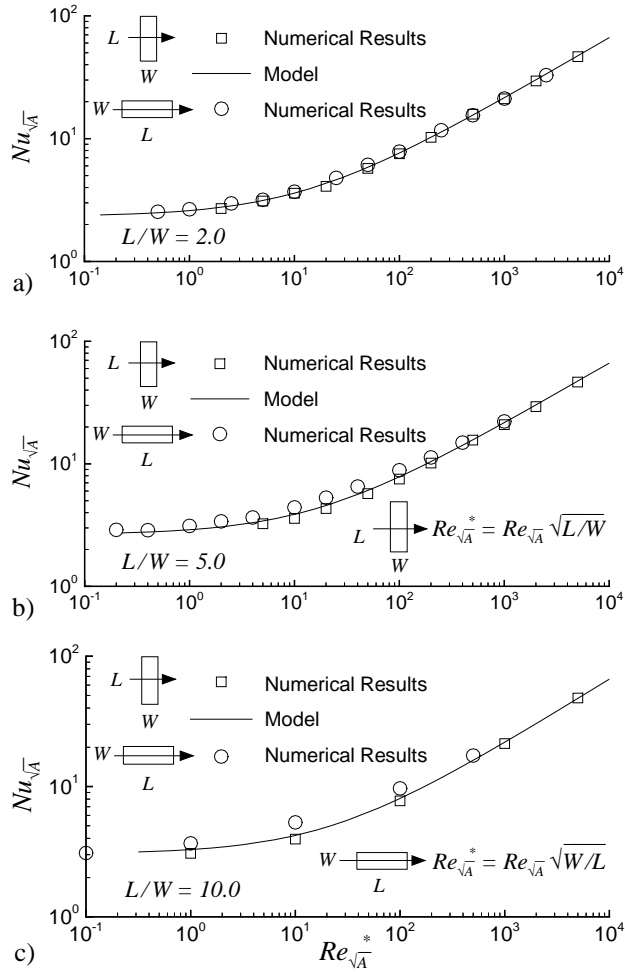


Fig. 5 Comparison of data and model:

- a)  $L/W = 2.0$
- b)  $L/W = 5.0$
- c)  $L/W = 10.0$

the majority of test cases, including all aspect ratio cases for flow in the  $W$ -direction and  $L/W \leq 2$  with flow in the  $L$ -direction, are in excellent agreement with the proposed model when  $n = 1.42$ . The only substantial differences between the model and the data occur in the transition region for the large aspect ratio rectangles,  $L/W = 5.0$  and  $10.0$ , with flow parallel to the long plate dimension  $L$ .

Figure 5 compares the proposed model using a fixed value of the interpolation parameter  $n = 1.42$  with the CFD data for three aspect ratios,  $L/W = 2.0, 5.0$  and  $10.0$ , for flow in both directions. In Fig. 5a the numerical results for  $L/W = 2.0$  with flow parallel to long and short plate dimensions are compared with the model. Through the use of the square root of area as the characteristic length in  $Nu_{\sqrt{A}}$ ,  $S_{\sqrt{A}}^*$ , the modified Reynolds number  $Re_{\sqrt{A}}^*$ ,

and the fixed value of the interpolation parameter, the model is independent of flow direction and can be represented on the plot by a single curve. The data in Fig. 5a also approach common asymptotes for large and small  $Re_{\sqrt{A}}^*$ , but show small deviations of approximately 2 - 3% between the results for the two flow directions in the intermediate region,  $Re_{\sqrt{A}}^* \approx 10$ .

The variations between the numerical data for the two flow directions is more evident for the  $L/W = 5.0$  case, with a maximum difference of 20% at  $Re_{\sqrt{A}}^* = 10$  as shown in Fig. 5b. These differences in the data for flow parallel to the long plate dimension  $L$  and flow along the short dimension  $W$  are the result of edge effects not accounted for in the proposed model. For the finite plate, the boundary layer tends to become thinner near the edges due to diffusion perpendicular to the flow direction, leading to enhanced heat transfer in these regions. This effect is most evident in the intermediate region,  $5 \leq Re_{\sqrt{A}}^* \leq 50$ , where boundary growth occurs quickly and the heat transfer is not conduction-dominated. The edge effects tend to enhance heat transfer in cases where the bulk fluid velocity is parallel to the long plate dimension  $L$ , while the effects are minimized in cases with flow along the short plate dimension  $W$ , resulting in a lower  $Nu_{\sqrt{A}}$ . With a fixed value for the interpolation parameter,  $n = 1.42$ , the model passes between the data, 7% above the lower data set and 13% below the upper data set at  $Re_{\sqrt{A}}^* = 10$ .

In Fig. 5c the model with  $n = 1.42$  for  $L/W = 10$  once again passes through the middle of the numerical data for flow in the  $L$ - and  $W$ -directions. The variation between the data in the intermediate region for the two flow directions is the largest of the three cases, due to the increase in edge effects for the larger aspect ratio. The model underpredicts the data for flow parallel to the long plate dimension  $L$  by a maximum of 26% at  $Re_{\sqrt{A}}^* = 10$ , and over-predicts the data for flow in the  $W$  direction by a maximum of 6% at  $Re_{\sqrt{A}}^* = 10$ .

In general, the proposed model is in close agreement, within 6 - 7%, of all the data for flow in the  $W$ -direction and  $L/W \leq 2$  for flow in the  $L$ -direction. The differences between the data and the model for  $L/W = 5.0$  and  $10.0$  is larger in the transition region due to edge effects.

Figures 6, 7 and 8 present temperature distributions in the region surrounding the plate using data from the CFD simulations. Each of these figures contain two sets of temperature contours: a) isotherms in an  $xy$ -plane along the midplane of the

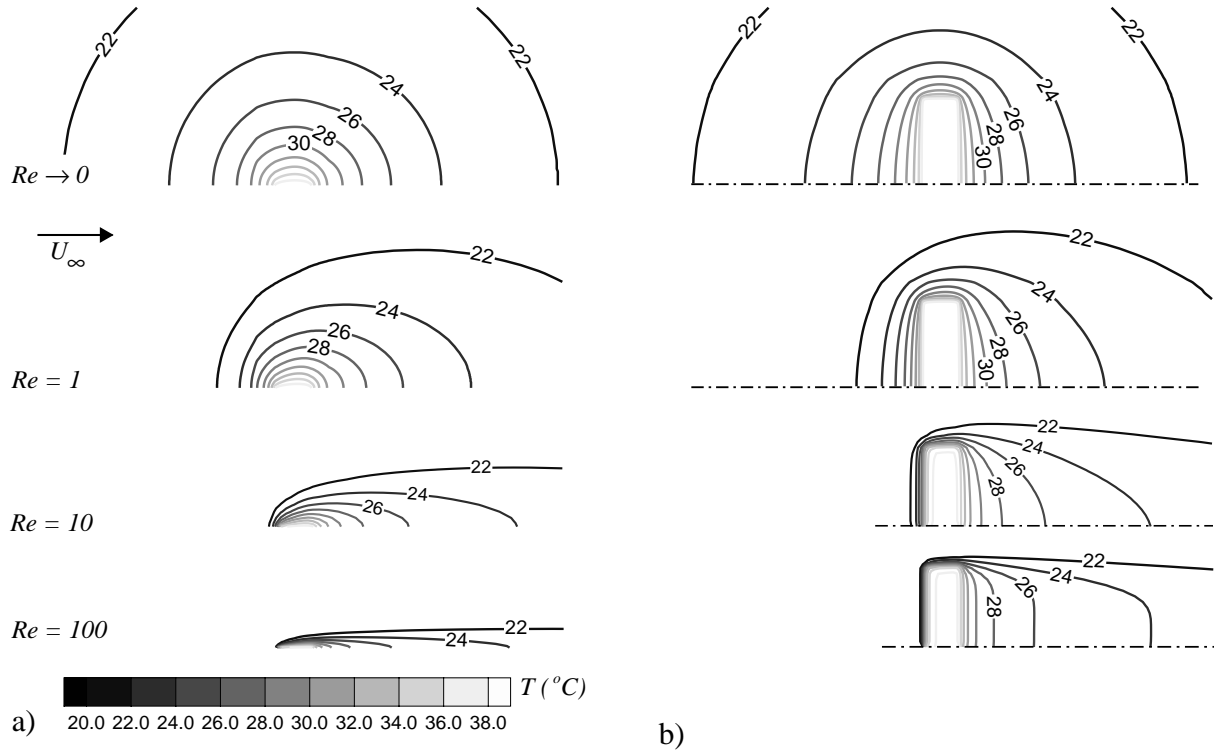


Fig. 6 Temperature distribution for  $L/W = 5.0$  with flow in  $W$ -direction:  
 a) midplane,  $z = L/2$ , b) plate surface,  $y = 0$

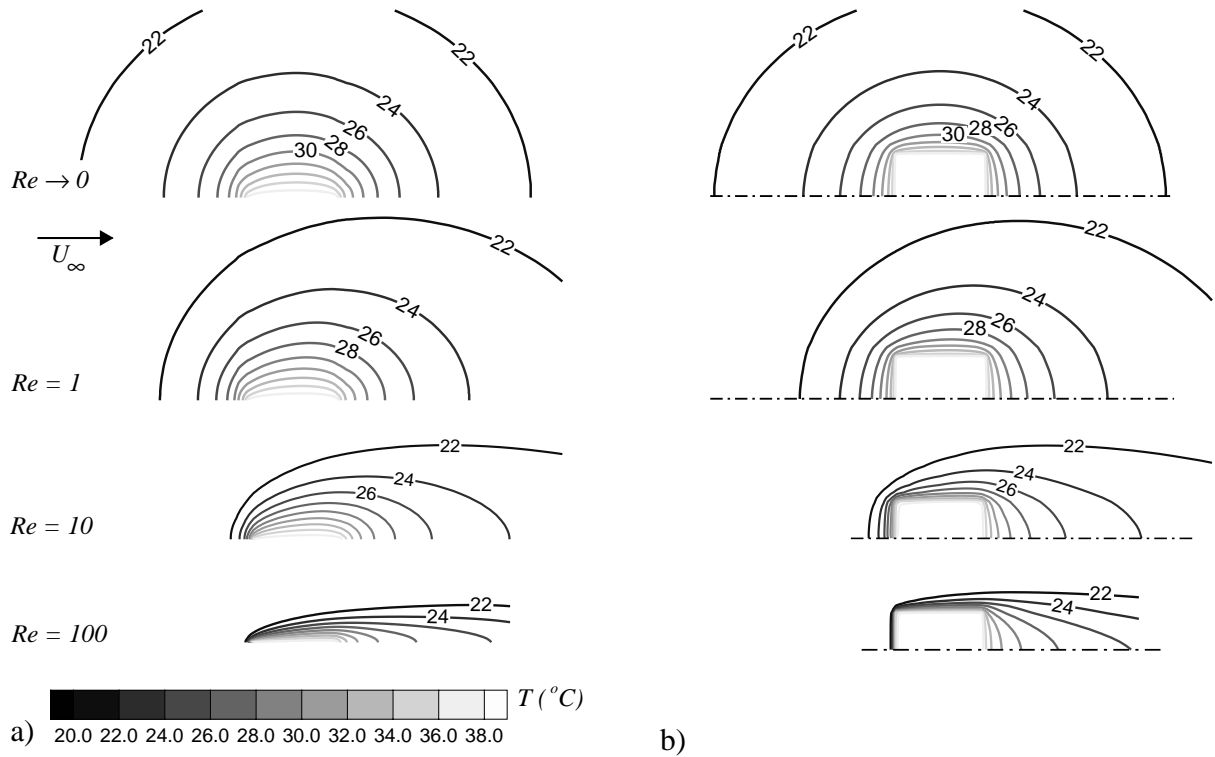


Fig. 7 Temperature distribution for  $L/W = 1.0$ : a) midplane,  $z = W/2$ , b) plate surface,  $y = 0$

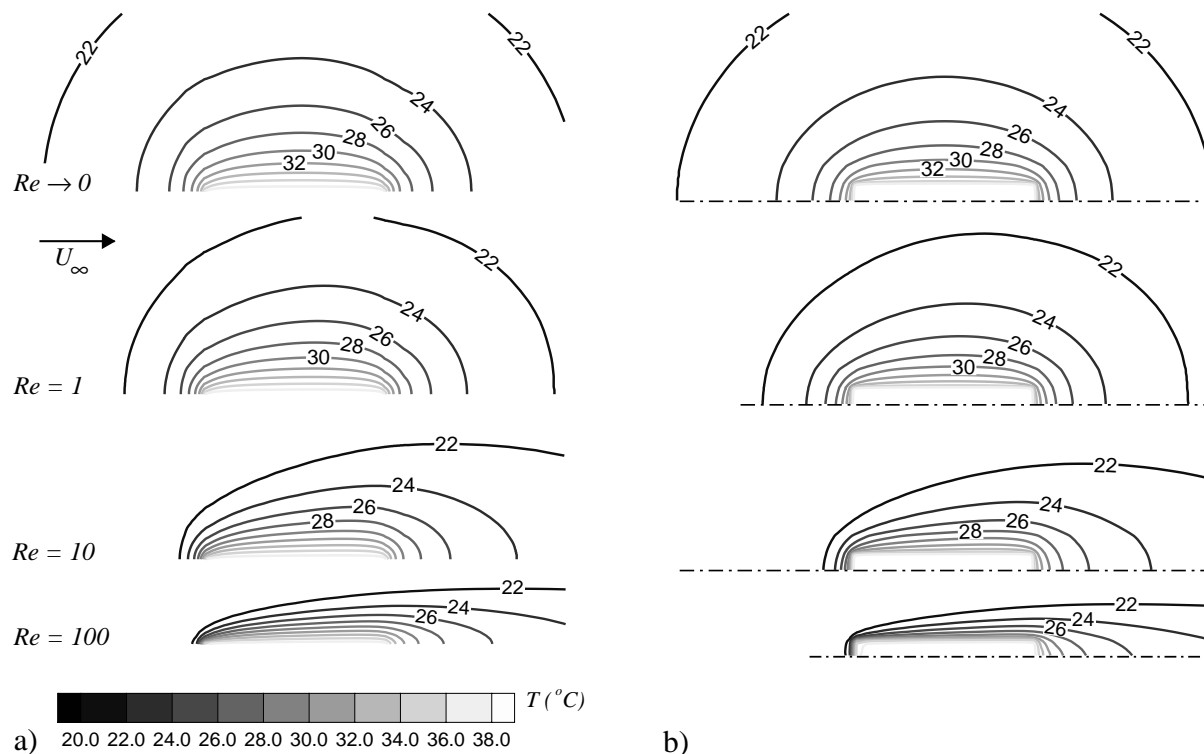


Fig. 8 Temperature distribution for  $L/W = 5.0$  with flow in  $L$ -direction:  
a) midplane,  $z = W/2$ , b) plate surface,  $y = 0$

plate,  $z = W/2$  or  $z = L/2$ ; and b) isotherms in the  $xz$ -plane at the plate surface,  $y = 0$ . Four different flow rates are plotted in each set, starting with the diffusive limit,  $Re \rightarrow 0$ , followed by  $Re = 1, 10$  and  $100$ , where  $Re$  is defined by Eqs. (23) and (25).

Each of the sets of contour plots presented in Figs. 6 - 8 clearly demonstrate the smooth transition between conduction-dominated (zero flow) and boundary layer flow. At the diffusive limit the isotherms extend radially outward from the plate, quickly becoming spherical-shaped contours consistent with pure conduction into a half-space. As flow is introduced, the free stream velocity begins to effect the temperature distribution. At  $Re = 1$  the isotherms near the plate still resemble those in the diffusion problem, but the outer isotherms are distorted by the free stream velocity. At  $Re = 10$  the advection effects become stronger, a distinct thermal boundary layer begins to form, and the problem begins to display two-dimensional characteristics. Finally, at  $Re = 100$ , two-dimensional boundary layer behavior has clearly been established, and diffusion in the  $z$ -direction perpendicular to the flow is minimized.

From the temperature contours for  $L/W = 5.0$  shown in Figs. 6 and 8 it appears that transition

from diffusion to boundary layer flow occurs more slowly for flow in the  $L$ -direction than for flow in the  $W$ -direction. If the isotherms for  $Re = 100$  are compared for each flow direction it is seen that the penetration of the temperature field into the fluid is much larger in Fig. 8 for flow in the  $L$ -direction than in Fig. 6.

This behavior can be attributed to the use of the plate side dimensions as the characteristic length in  $Re$ . For each  $L/W = 5.0$  case, the value  $Re = 100$  can be recast in terms of the modified Reynolds number,  $Re^*_{\sqrt{A}}$  defined previously. For flow parallel to the short plate dimension  $W$ , as shown in Fig. 6:

$$Re = 100, \quad Re^*_{\sqrt{A}} = 500$$

and for flow in the  $L$ -direction, as shown in Fig. 8:

$$Re = 100, \quad Re^*_{\sqrt{A}} = 20$$

Based on these values for the modified Reynolds number it can be concluded that at  $Re=100$  the  $L/W = 5.0$  case shown in Fig. 8 is in the middle of the transition region, while the same case in Fig. 6 behaves according to the two-dimensional, boundary layer solution.

## Summary and Conclusions

A composite correlation equation has been developed that accurately predicts the average Nusselt number for laminar forced convection heat transfer from isothermal finite rectangular plates. The proposed model is valid for all fluids  $Pr > 0.5$  and for a wide range of the Reynolds number  $0 < Re_L < 5000$  for flow in both the  $W$ - and  $L$ -directions.

It has been demonstrated that the use of the square root of the active surface area as the scale length in the dimensionless parameters reduces the effects of aspect ratio and flow direction on the solution. Using  $\sqrt{A}$  as the characteristic length in the correlation equation reduces the range of the interpolation parameter to a single value for all aspect ratios and flow directions.

Accurate numerical results have been presented for the Nusselt number for the aspect ratios  $L/W = 1.0, 2.0, 5.0$  and  $10.0$  in the range  $0 < Re < 5000$  with flow in both the  $W$ - and  $L$ - directions. When the plate side length,  $L$  or  $W$ , is used as the scale length, and the interpolation parameter is determined using the correlations provided, the agreement between the proposed model and the data is excellent, with a maximum percent difference of 4.5% and an RMS percent difference of 1.9%.

Contour plots for the temperature distribution in the region surrounding the plate have been generated using the data from the CFD simulations, and are presented for three cases. The isotherms in these contour plots clearly demonstrate the smooth transition between the diffusive limit,  $Re \rightarrow 0$ , and the two dimensional, laminar boundary layer solution.

## Acknowledgments

The first author acknowledges the financial support of the Natural Sciences and Engineering Research Council of Canada under Grant A7455. The authors also thank Materials and Manufacturing Ontario for their continued support.

## References

- <sup>1</sup> Schlichting, H., *Boundary Layer Theory*, 6th ed., McGraw-Hill, New York, 1968.
- <sup>2</sup> Knudsen, J., and Katz, D., *Fluid Dynamics and Heat Transfer*, McGraw-Hill, New York, 1958.
- <sup>3</sup> Kays, W.M., and Crawford, M.E., *Convection Heat and Mass Transfer*, 2nd ed., McGraw-Hill, New York, 1980.
- <sup>4</sup> Schetz, J.A., *Boundary Layer Analysis*, Prentice-Hall, New Jersey, 1993.
- <sup>5</sup> Refai Ahmed, G., and Yovanovich, M.M., "Analytical Method for Forced Convection from Flat Plates, Circular Cylinders, and Spheres," *J. of Thermophysics and Heat Transfer*, Vol. 9, No. 3, 1995, pp. 516-523.
- <sup>6</sup> Yovanovich, M.M., "Dimensionless Shape Factors and Diffusion Lengths of Three-Dimensional Bodies," *Proceedings of the ASME/JSME Thermal Engineering Joint Conference*, Vol. 1, 1995, pp. 103-113.
- <sup>7</sup> Schneider, G.E., "Thermal Resistance Due to Arbitrary Dirichlet Contacts on a Half-Space," *AIAA Prog. in Astro. and Aeronautics: Thermophysics and Thermal Control*, Vol. 65, 1978, pp. 103-119.
- <sup>8</sup> Yovanovich, M.M., Lee, S., and Gayowsky, T.J., "Approximate Analytical Solution of Laminar Forced Convection from an Isothermal Plate," AIAA Paper 92-0248, 30th Aerospace Sciences Meeting and Exhibit, Reno, NV, January 6 - 9, 1992.
- <sup>9</sup> Churchill, S.W., and Usagi, R., "A General Expression for the Correlation of Rates of Transfer and Other Phenomena," *AIChE Journal*, Vol. 18, 1972, pp. 1121-1128.
- <sup>10</sup> Flomerics Inc., 2 Mount Royal Ave., Marlborough, MA, 1998.